CHALMERS
UNIVERSITY OF TECHNOLOGY

Loudspeaker parameter identification for automatic fault detection

Modelling and identification of the impedance of a loudspeaker for automatic fault detection in power amplifiers

Master's thesis in Systems, Control and Mechatronics

PHILIP LARSSON

Loudspeaker parameter identification for automatic fault detection

Modelling and identification of the impedance of a loudspeaker for automatic fault detection in power amplifiers

PHILIP LARSSON

Loudspeaker parameter identification for automatic fault detection
Modelling and identification of the impedance of a loudspeaker for automatic fault detection in power amplifiers
PHILIP LARSSON

Supervisor: Jonas Sjöberg, Department of Electrical Engineering
Advisor: Marco Monzani, LAB.GRUPPEN
Examiner: Jonas Sjöberg, Department of Electrical Engineering

Cover:

Loudspeaker parameter identification for automatic fault detection
Modelling and identification of the impedance of a loudspeaker for automatic fault
detection in power amplifiers
PHILIP LARSSON
Department of Electrical Engineering
Chalmers University of Technology

Abstract

Detecting the presence of a load connected to a power amplifier in audio applications
is typically done using specific test signals during operation. This method provides
no indicators whether the impedance profile of the load has changed due to damage
or aging and the test signals can cause audible distortions when the amplifier is used
for playing music. This thesis investigates the use of a system identification approach
to identify defects and irregular behaviour in loudspeakers using parameter identi-
fication and impedance profiling. This is done by conducting voltage and current
measurements on three loudspeakers before and after imposing common defects on
the units. The study shows that the damping ratio and resonance frequency of the
loudspeaker units deviate significantly due to the investigated failure modes. Using
the proposed fault detection implementations of this thesis, these failure modes can
be detected with low complexity algorithms by measuring the voltage and current
of the power amplifier output during normal operation and thus remove the need
for test signals.

Acknowledgements

I would like to thank LAB.GRUPPEN and my company supervisor Marco Monzani for giving me the opportunity to work on this thesis project. I would also like to thank my supervisor at Chalmers, Jonas Sjöberg, for his knowledge and advice during the project.

Contents

Contents

List of Figures

List of Tables

1

Introduction

This chapter will provide an introduction to the project by discussing the background behind the problem proposed by the company, the contribution of the study's findings to existing research and the general approach used to reach the results of the project.

1.1 Background

Power amplifiers used for audio applications are designed to power loudspeakers or headphones. To ensure that a load (normally a loudspeaker) is connected to the output of the amplifier and that the electric circuit is actually closed, the amplifier sends out specific test signals called "pilot tones" intermittently to check. These pilot tones are usually outside of audible range, e.g. ~ 10 Hz or ~ 30 kHz, and are required by normative if the amplifier is to be used in a voice evacuation system. The use of pilot tones however only provides the knowledge that the loudspeaker unit is disconnected, returning no other information about the state or possible damage to the unit, and they can cause audible harmonic overtones when used while playing music. Moreover, a limitation of the pilot tones is that they are unable to traverse passive cross-over filters possibly embedded in some loudspeaker cabinets.

An alternative to the use of pilot tones would be to measure the impedance as seen by the amplifier during operation and use this information to detect any sign of loudspeaker malfunction. The intended output of the amplifier (e.g. music or recorded voice messages) could then be used as the test signal and no pilot tones would be needed. The audible program content typically covers a broad frequency range, and is possibly more suitable for the purpose of diagnosing loudspeakers and to identify deviations in loudspeaker operation than pilot tones. Such deviations may indicate that the loudspeaker is going to fail, and therefore makes it possible to take proper countermeasures before the event actually occurs. This could be crucial in the use of an amplifier in a voice evacuation system, where recorded spoken messages are used to evacuate people in the case of an emergency.

The frequency dependent complex impedance of a loudspeaker has an amplitude curve with one prominent resonance peak (typically several in the case of loudspeakers mounted into cabinets) and an inductive rise at higher frequencies. The appearance of this amplitude curve is very different depending on the parameters of the speaker (e.g. mechanical resistance, suspension compliance etc.), which opens up

to the possibility of relating specific impedance profiles to certain abnormal speaker behaviours. For example, overheating of the voice coil in the loudspeaker - the element that creates a magnetic field proportional to the electric current - induces variations in this magnetic field which in turn affects the impedance profile, often by shifting the resonance frequency and changing the amplitude of the resonance peak. By identifying the relation between a certain parameter change in the impedance model and a certain loudspeaker defect, the user can be notified about the need to reduce the power delivered to a loudspeaker to avoid further degeneration, or to replace the element. If the speaker is to be replaced, but has not failed yet, it may be also possible to log the condition in which the speaker was brought to failure - which may have disappeared after a complete failure.

1.2   LAB.GRUPPEN

LAB.GRUPPEN is a company located in Kungsbacka, Sweden, developing power amplifiers and DSP-units (Digital Signal Processing) for PA-systems (Public Address). Their equipment is commonly used in venues and arenas where the requirement for power output is high, but also in voice evacuation systems.

The company's wished outcome of the project was to replace pilot tones and their previously mentioned disadvantages with an alternative, to enable preventive diagnostics of the load connected to the power amplifier and to improve the reliability of audio systems in safety critical applications such as voice evacuation systems. All of these items are touched upon in this thesis.

1.3   Contributions to existing research

The contribution of this study to previous research is the investigation of the parameter variations related to consumer-side defects in loudspeakers. While there are studies presenting the physical parameter deviation due to temperature increase in the voice coil [1] and large voice coil excursions [2], there exists a gap in published research regarding the deviation due to breakdown or irregular behaviour in loudspeaker units, emanating from prolonged use.

Methods for identifying defects in loudspeakers originating from production has been developed using sound pressure measurements at the production line [3]. Furthermore, online fault detection has been covered several times for the use in HVAC-systems using system identification approaches similar to the methods used in this study [4]. This study thus bridges the gap of the research in these areas and combines the ideas and findings for the use in a new application.

This thesis also extends the research done on temperature drift in loudspeaker parameters in [1] and [5] and utilizes methods of loudspeaker system identification developed in [6], [5] and [7] to propose a low complexity fault detection system able to replace the use of pilot tones in power amplifiers.

1.4 Loudspeaker parameter identification approach

This section will discuss the general approach to the problem of the thesis project, while the "Methods" chapter will go into further into the details of each process.

By measuring the current, voltage and the temperature of the voice coil, the Thiele/Small parameters of the loudspeaker was identified using various loudspeaker models. This identification procedure was performed on functioning loudspeaker units and compared with the identified parameters of the same loudspeaker unit after imposing defects using destructive methods. The changes in the parameter values due to a particular defect in the loudspeaker was investigated and methods for identifying the parameter changes online by the power amplifier was proposed.

1.5 Outline of the thesis

This thesis report is divided into six chapters. An introduction to the theory behind the methods used is provided in Chapter 2, where details on loudspeaker impedance models, modelling approaches and failure modes of loudspeakers are given. The influence of previous studies on the chosen methods in this thesis project is also discussed.

Chapter 3 follows up with the practical details behind the experiment design, data collection, system identification and implementation.

The results of the system identification and parameter analysis is presented in Chapter 4.

Implementation aspects, limitations of the study and suggestions for future work is then presented in Chapter 5.

The thesis report is then rounded off in Chapter 6, where the entire findings of the study is summarized.

2

Theory

2.1   The moving coil loudspeaker

A loudspeaker is an electroacoustic transducer that converts electrical energy into air pressure. In a moving coil loudspeaker, voltage applied to the terminals causes a current to pass through a coil in the loudspeaker unit known as the voice coil. The voice coil, located inside of the permanent magnetic field of the loudspeaker magnet (see Fig 2.1), then produces a magnetic field perpendicular to the current and magnetic field of the magnet. This generates a mechanical force that moves the voice coil back and forth on its axis. The movement of the voice coil causes the connected diaphragm to move the air around it, creating sound [8].

The voice coil is kept in place by the suspension, comprising of the spider and the surround. This allows the voice coil to move freely in the gap between the front plate and the pole piece. The front plate, pole piece and back plate are made of highly permeable metals, usually iron, thus guiding the magnetic field to intensify in the gap where the voice coil travels. In Figure 2.1, the front plate can be seen located between the magnet and the frame and the back plate is here fused together with the pole piece on the back of the loudspeaker.

For small signal levels, the moving coil loudspeaker exhibits fairly linear behaviour [9]. Small displacements of the voice coil inside the homogeneous magnetic field of the gap allows the use of a linear equivalent electrical circuit to model the behaviour of the loudspeaker. The most common model is known as the Thiele/Small model, named after Neville Thiele and Richard H. Small who derived the model in the seventies [10]. The linear parameters of this electromechanical circuit are still widely used for loudspeaker and enclosure design today. Several modifications to the Thiele/Small model has been proposed over the years, one common being the LR-2 model, where the effect of eddy currents induced in the pole structure has been considered [11]. The Thiele/Small model and its related parameters are however only valid closely around a specific operating point of the diaphragm position, and does not accurately describe the normal operation of a loudspeaker. As the input voltage across the loudspeaker terminals increases, the voice coil excursions become bigger, causing parts of the coil to leave the homogeneity of the field gap, thus entering the nonlinear region of operation [9].
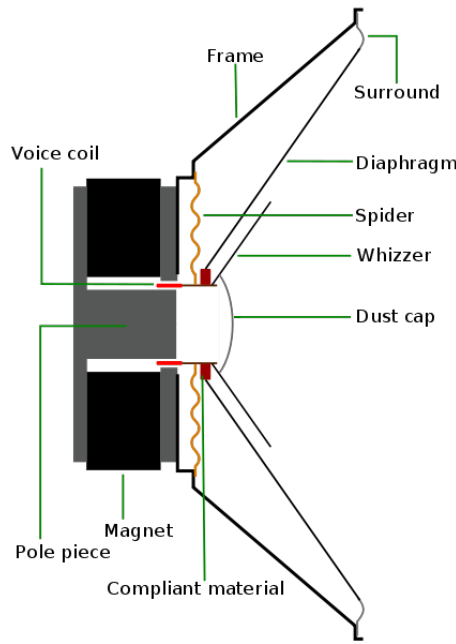
Figure 2.1: Mechanical structure of a moving coil loudspeaker [12]

2.1.1 Linear transducer model

The equation for the electrical part of the lumped electro-mechanical Thiele/Small-model (see Figure 2.2) can be derived using Kirchhoff's voltage law,

$$u(t) = R_e i(t) + L_e \frac{\mathrm{d}i(t)}{\mathrm{d}t} + Bl \cdot v(t) \tag{2.1}$$

where $u(t)$ is the input voltage of the loudspeaker, $i(t)$ is the current, $v(t)$ is the velocity of the loudspeaker diaphragm, R_e is the voice coil resistance, L_e is the voice coil inductance and Bl is the force factor. This last term, measured in Tesla meters, is the term describing the force applied to the voice coil by the magnetic field as current flows through the coil.

The mechanical part of the linear lumped loudspeaker model can be derived using Newton's laws of motion. The force applied to the loudspeaker cone is counteracted by the mass of the cone, the suspension stiffness (reciprocal of compliance) and mechanical losses,

$$F(t) = Ma(t) + R_{ms}v(t) + \frac{1}{C_{ms}}x(t) \tag{2.2}$$

where $a(t)$ is the acceleration of the diaphragm, $x(t)$ is the position of the diaphragm, $F(t)$ is the driving force applied to the voice coil, M is the moving mass of the loudspeaker, R_{ms} is the mechanical resistance due to losses and C_{ms} is the compliance

of the suspension.

Since the magnetic field of the voice coil generates a force as current is applied to it, the two equations above can be connected using the force factor Bl [13]:

$$F(t) = Bl \cdot i(t) \tag{2.3}$$

By Laplace-transforming this system of equations, a transfer function for the impedance of the loudspeaker can be derived:

$$H_I(s) = \frac{U(s)}{I(s)} = \frac{s^2 + \frac{Bl^2 + (R_e + sL_e)R_{ms}}{M(R_e + sL_e)}s + \frac{1}{MC_{ms}}}{\frac{1}{R_e + sL_e}\left(s^2 + \frac{R_{ms}}{M}s + \frac{1}{MC_{ms}}\right)} \tag{2.4}$$

As can be seen by multiplying the numerator and denominator of (2.4) by "$R_e + sL_e$", this impedance transfer function is improper, having more zeros than poles. This is circumvented by using the voltage as an input and the current as output, thus estimating the admittance instead of the impedance. For system identification, the voice coil inductance is often set to zero, leading to the following low-frequency transfer function:

$$H_I(s)|_{L_e=0} = \frac{s^2 + \frac{Bl^2 + R_e R_{ms}}{MR_e}s + \frac{1}{MC_{ms}}}{\frac{1}{R_e}\left(s^2 + \frac{R_{ms}}{M}s + \frac{1}{MC_{ms}}\right)} \tag{2.5}$$

In order to model the high frequency behaviour of the loudspeaker, extensions to the equivalent electrical circuit can be seen in Figure 2.2.
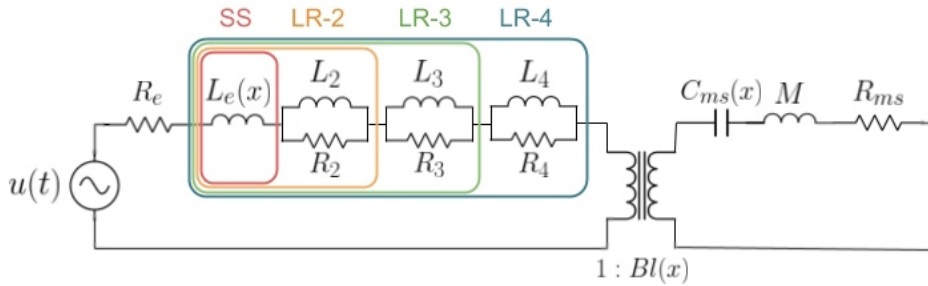
Figure 2.2: Equivalent electrical circuit of the moving coil loudspeaker with the cascaded LR-networks of the various model structures.

Introducing the voice coil inductance into the model, the following state space model can be used to estimate the admittance of the loudspeaker:

$$\dot{\boldsymbol{x}}(t) = \begin{bmatrix} \frac{-R_{ms}}{M} & \frac{-1}{MC_{ms}} & \frac{Bl}{M} \\ 1 & 0 & 0 \\ \frac{-Bl}{L_e} & 0 & \frac{-R_e}{L_e} \end{bmatrix} \boldsymbol{x}(t) + \begin{bmatrix} 0 \\ 0 \\ \frac{1}{L_e} \end{bmatrix} u(t) \tag{2.6}$$

$$y(t) = \begin{bmatrix} 0 & 0 & 1 \end{bmatrix} \boldsymbol{x}(t) \tag{2.7}$$

where the state vector $\boldsymbol{x}$ is defined as $\boldsymbol{x} = [\dot{x} \ \ x \ \ i]$. This is the model that can be seen as "SS" in Figure 2.2.

At very high frequencies, the eddy currents induced in the pole structure cause an inductive rise in the impedance of the loudspeaker. This is commonly modelled using an inductor and a resistor in parallel (see Figure 2.2). Introducing the current through the inductor L_2, $i_2(t)$, as a fourth state results in the following state space model:

$$\dot{\boldsymbol{x}}(t) = \begin{bmatrix} \frac{-R_{ms}}{M} & \frac{-1}{MC_{ms}} & \frac{Bl}{M} & 0 \\ 1 & 0 & 0 & 0 \\ \frac{-Bl}{L_e} & 0 & \frac{-(R_e+R_2)}{L_e} & \frac{R_2}{L_e} \\ 0 & 0 & \frac{R_2}{L_2} & \frac{-R_2}{L_2} \end{bmatrix} \boldsymbol{x}(t) + \begin{bmatrix} 0 \\ 0 \\ \frac{1}{L_e} \\ 0 \end{bmatrix} u(t) \tag{2.8}$$

This model is often referred to as the "LR-2 model" and can be extended to higher order models such as the LR-3 and LR-4 by cascading several LR-networks as in Figure 2.2.

2.1.2 Nonlinearities

The nonlinearities affecting the loudspeaker behaviour the most is the voice coil position dependence of the force factor, $Bl(x)$, compliance of the suspension, $C_{ms}(x)$ and inductance of the voice coil, $L_e(x)$ [14]. Here x denotes the displacement of the voice coil and subsequently the diaphragm.

As the voice coil moves out of the field gap, the force imposed on the coil decreases, lowering the value of $Bl(x)$. This voice coil displacement dependence is generally symmetrical, and is often modelled as a Gaussian sum or as a polynomial expansion. The advantage of the Gaussian sum being the avoidance of negative values for large excursions.

The compliance $C_{ms}(x)$ of the suspension exhibits a similar symmetric behaviour. As the voice coil moves far out of the field gap, the suspension, i.e. the surround and spider, act as a nonlinear spring, becoming stiffer as the voice coil ventures from its operating point. This nonlinearity, having similar behaviour to the force factor, is also often modelled as Gaussian sum.

The third major nonlinearity, the voice coil inductance $L_e(x)$, has a different behaviour. As the voice coil displacement increases (here meaning away from the magnet, towards the cone), the inductance decreases. Conversely, the inductance

increases with negative displacement. This is due to the permeability of the material around the coil at the different positions. The voice coil inductance is often modelled as a sigmoid function [7].

Fortunately, as the force factor, suspension compliance and voice coil inductance are constant parameters in the lumped electromechanical Thiele/Small model, these nonlinearities can simply be substituted into the mathematical equations of the model. The three constant parameters in the linear model can thus be replaced with the the following terms:

$$Bl(x) = \sum_{n=1}^{N} a_n e^{-\frac{(x-x_{n,a})^2}{2\sigma_a^2}} \tag{2.9}$$

$$C_{ms}(x) = \sum_{n=1}^{N} b_n e^{-\frac{(x-x_{n,b})^2}{2\sigma_b^2}} \tag{2.10}$$

$$L_e(x) = \frac{L_1}{1 + e^{-c(x-x_0)}} + L_0 \tag{2.11}$$

2.1.3 Frequency dependence of parameters

Five of the six Thiele/Small-parameters are directly related to the Q factor, i.e. the parameter describing the damping of a resonator, and the frequency of the loudspeaker resonance

$$f_n = \frac{1}{2\pi\sqrt{C_{ms} \cdot M}} \tag{2.12}$$

$$Q_{es} = \frac{2\pi \cdot f_n \cdot M \cdot R_e}{Bl^2} \tag{2.13}$$

$$Q_{ms} = \frac{2\pi \cdot f_n \cdot M}{R_{ms}} \tag{2.14}$$

$$Q = \frac{Q_{ms} \cdot Q_{es}}{Q_{ms} + Q_{es}} \tag{2.15}$$

where Q_{ms} is the mechanical Q factor, Q_{es} is the electrical Q factor, Q is the total Q factor of the driver and f_n is the undamped natural frequency [15].

For second order systems in standard form, e.g. (2.5), the damping ratio is a more commonly used metric of the damping of a system:

$$\zeta = \frac{1}{2Q} \tag{2.16}$$

Since the Q factor in turn is related to the bandwidth of the resonance peak, these five parameters are typically identifiable using an input signal with frequencies lower

than 100 Hz for a medium to large sized driver.

Since the DC-resistance parameter R_e is related to the impedance at DC-excitation (0 Hz), input signals for system identification need to contain very low frequencies in order to achieve accurate estimations of this parameter.

2.1.4   Temperature dependence of parameters

Since the efficiency of a common loudspeaker ranges between 0.5 % to 2 % [16], the majority of the power is converted into heat. As the temperature increases during use, the electrical equivalent Thiele/Small parameters of the loudspeaker starts to drift. In [1] the temperature drift of the loudspeaker parameters was investigated on a car loudspeaker. The linear parameters found to be affected by a temperature increase from 20° C to 80° C was the voice coil resistance R_e, the force factor Bl, the moving mass M, the suspension compliance C_{ms} and the mechanical resistance R_{ms}. The changes in the parameters ranged from a relatively small increase in the suspension compliance by 9 % to a decrease in the mechanical resistance by 42 %.

Resistance in a conductor due to increased temperature is often approximated using the following linear model:

$$R_e(T_e) = R_e(T_0)(1 + \alpha(T_e - T_0)) \tag{2.17}$$

where T_0 is the ambient temperature and α is the temperature coefficient of the conductive material, in the case of a loudspeaker typically copper.

The reason behind investigating parameter drift due to temperature in this thesis project is the magnitude of the changes observed in [1]. A small parameter variation due to a defect in the loudspeaker unit could easily be overshadowed by the variations due to temperature. Furthermore, a parameter variation due to temperature could be wrongfully detected as a defect in the loudspeaker if this is not accounted for in the fault detection system.

2.2   System identification

Model estimation in system identification can be divided into two groups of methods, online and offline. The offline system identification procedures estimates the parameters of the model based on a number of data points from measurements, while online methods are usually limited to the the last measured sample in an observed system.

Working on a larger set of data, the offline methods are superior in terms of model fit and stability, but these methods are seldom practical to use in the integrated software of a product due to possible time-varying behaviour in the identified system and the methods being computationally expensive. The choice between these two methods thus comes down to the rate of parameter drift in the system and the

available processing power of the platform running the software.

In this thesis project, the main method of choice for the modelling and parameter deviation analysis was the offline grey-box modelling approach. For the analysis of the parameter changes in relation to defects, the offline approach, working on a larger set of data, provides more accurate estimation results. In regards to the detection of faults however, some defects are likely to occur slowly over time while others might be more sporadic. For this reason, the proposed implementation of fault detecting systems in this study utilized the online estimation approach.

As there exists a number of mathematical models of the loudspeaker containing the physical parameters of the system, the grey-box approach for the theoretical part of the thesis becomes the obvious choice given this insight in the physical system. This analysis is also what weighs more heavily in this thesis project in terms of academic value. For the implementation aspect of the project however, black-box models was utilized due to their low complexity and resemblance to digital filters.

2.2.1 Offline Modelling

Conventional system identification procedures involve the minimization of the prediction error, known as the Prediction Error Method (PEM). The prediction error, $\varepsilon(t, \boldsymbol{\theta})$, is the difference between the one-step model prediction, $\hat{y}(t|t-1, \boldsymbol{\theta})$, and the observed output, $y(t)$ at time t:

$$\varepsilon(t, \boldsymbol{\theta}) = y(t) - \hat{y}(t|t-1, \boldsymbol{\theta}) \tag{2.18}$$

Using a positive, scalar function, l, the optimization problem becomes the problem of minimizing the loss function $V_N(\boldsymbol{\theta})$:

$$\hat{\boldsymbol{\theta}}_N = \arg\min_{\boldsymbol{\theta} \in S} V_N(\boldsymbol{\theta}) = \arg\min_{\boldsymbol{\theta} \in S} \frac{1}{N} \sum l(t, \boldsymbol{\theta}, \varepsilon(t, \theta)) \tag{2.19}$$

Commonly, the scalar function l is chosen as $l(t, \boldsymbol{\theta}, \varepsilon(t, \boldsymbol{\theta})) = \varepsilon^2(t, \boldsymbol{\theta})$. This is also what is used for the PEM in MATLAB. The solution to this optimization problem is the parameter vector $\hat{\boldsymbol{\theta}}_N$ which is an estimator of the true system parameters $\boldsymbol{\theta}$ [17].

2.2.2 Recursive model estimation

By mapping the poles of a second order system to the z-plane ($z = e^{sT_s}$), the coefficients of the discrete time z-transform representation in standard form,

$$H(z) = \frac{b_1 z^{-1}}{1 + a_1 z^{-1} + a_2 z^{-2}} \tag{2.20}$$

can be used to calculate the poles of the original system. The advantage to this method is that a discrete time system such as (2.20) easily can be estimated recursively online. Using trigonometrics, the poles of the original system can be reconstructed from the digital filter coefficients as

$$s_{p1}, s_{p2} = f_s \left(\ln(\sqrt{a_2}) \pm i \cdot \tan^{-1} \left(\frac{\sqrt{-a_1^2 + 4a_2}}{a_1} \right) \right) \qquad (2.21)$$

where f_s is the sampling frequency of the system. The magnitude of the poles of the standard form polynomial corresponds to the natural frequency of the system, $\omega_n = |s_{p1}|$, and the damping ratio can be found as

$$\zeta = \frac{-\ln(\sqrt{a_2})}{\omega_n T_s} \qquad (2.22)$$

as seen in [6], where T_s is the sampling period of the system.

Choosing a model structure such as an ARMAX or OE with two poles, the parameters a_1 and a_2 can be estimated using the following recursive algorithm, minimizing the prediction error $\varepsilon(t) = y(t) - \hat{y}(t)$:

$$\hat{\boldsymbol{\theta}}(t) = \hat{\boldsymbol{\theta}}(t-1) + \boldsymbol{K}(t)(y(t) - \hat{y}(t)) \qquad (2.23)$$

where the gain $K(t)$ is calculated as:

$$\boldsymbol{K}(t) = \boldsymbol{Q}(t)\boldsymbol{\psi}(t) \qquad (2.24)$$

where $\boldsymbol{\psi}(t)$ is the gradient of the predicted model output $\hat{y}(t, \boldsymbol{\theta})$ with respect to the parameter vector $\boldsymbol{\theta}(t)$. $\boldsymbol{Q}(t)$ is calculated differently based on the chosen method. Methods supported by the System Identification Toolbox (SITB) in MATLAB include the forgetting factor method, the Kalman filter method and the normalized and unnormalized gradient method [18].

2.2.3   Input signal for loudspeaker system identification

Although a sparse multi-tone sinusoid as recommended by Klippel and Schlecter in [20] could aid in distortion analysis, a noise signal such as a pink or a white noise exhibits the persistently exciting qualities needed for the identification of the many parameters in the loudspeaker grey-box model [21]. While full orchestral or pop music has been shown to be of persistently exciting nature [22], [6] shows that the convergence rate for such an input signal for parameter estimation is much slower than when using a broad band noise signal.

2.3 Loudspeaker failure modes

The failure modes of loudspeakers can be divided into two groups - mechanical failure and thermal failure. Some of the common loudspeaker defects are discussed below.

Voice coil rubbing can occur if the voice coil is misaligned. This can occur due to production errors or due to suspension failure, since the spider and the surround are responsible for securing the voice coil in the gap. This rubbing can cause audible distortion and will likely lead to failure of the loudspeaker unit if not seen to.

Voice coil bottoming is the phenomenon when the voice coil hits the back plate. This can occur if there is an offset of the voice coil from aging, climate or gravity and/or when the loudspeaker is driven beyond its limits in terms of input power. This defect will also likely lead to a complete failure after continued use.

Other mechanical defects include loose electrical connections, loose particles in the enclosure, air leaks, loose wire beating and excessive vibrations. Apart from the first, these defects are less likely to be detectable in the electrical domain than they are in the acoustical domain.

Thermal failure of the loudspeaker unit is typically due to voice coil overheating. While some of the heat generated is conducted to other parts of the loudspeaker through the air gap, the voice coil is the component that has to withstand most of the thermal load during use. Overheating of the voice coil can lead to immediate failure when adhesives and the coating of the copper wire start melting, but long-term non-destructive overheating can lead to the voice coil deforming, causing rubbing [19].

3

Loudspeaker impedance measurement and modelling

For the first part of the loudspeaker modelling, various input signals and model structures was compared by estimating the parameters of one of the loudspeaker units. The selected input signal and model structure was then used to estimate the parameters of the other loudspeaker units before and after imposing various defects. The second part involved investigating methods for detecting the identified parameter changes online in simulation.

3.1 Data collection

The measurements were conducted by exciting the loudspeaker units with a band-limited white Gaussian noise (WGN) signal while measuring the voltage at the loudspeaker terminals and the current passing through the loudspeaker. Using the recorded voltage signal as an input signal and the current signal as an output signal, the admittance (reciprocal of impedance) was estimated using grey-box model structures based on the equations presented in Chapter 2 in the System Identification Toolbox in MATLAB.

3.1.1 Equipment

For the data collection, the loudspeaker samples were attached to a robust wooden construction magnetically using a metal plate. The permanent magnet in the loudspeakers then kept the samples firmly attached to the construction by screws in the metal plate.

The measurements were done using an automated test rig located at LAB.GRUPPEN used for the testing of power amplifiers. The rig has a 14 channel FireWire connectable amplifier in-out recorder (AIOR) able to sample current and voltage at 48 kHz. This rig and the corresponding MATLAB-software was used to record and store the voltage and current signals into the MATLAB work space.

A power amplifier was used to generate the input excitation signal for the loudspeaker. The input signals were generated using MATLAB with the output of the computer sound card connected to the input of the power amplifier. The output

of the power amplifier was connected to the loudspeaker units via the AIOR sound card of the rig, allowing voltage and current to be measured.

3.1.2 Loudspeaker input signal

In order to find the input signal for parameter estimation and modelling resulting in parameter estimations as close to the true system parameters as possible, different frequency band noise signals was tested. 100,000 samples of each frequency band input signal was used for estimating the parameters of the model structures. The input signals were generated using a white Gaussian noise signal filtered using a low-pass filter with cutoff frequency $f_c = 100, 200, 300, 400, 500, 750, 1000, 2000, 10000$ and 20000 Hz. The motivation behind these choices of input signal frequency bands is the shape of the impedance magnitude of a loudspeaker. The impedance function $Z(f)$ is sensitive (i.e. $Z'(f)$ high) for frequencies around the resonance and around the high frequency rise, see Figure 3.1. It is thus important to spend a lot of input power in these frequency bands in order to model the loudspeaker dynamics properly.

The amplitude levels was chosen as the maximum level allowed by the power amplifier limiter (automatically lowering the gain once distortion is detected) and one at half of this level. Since nonlinear behaviour in the moving coil loudspeaker becomes prominent for larger amplitudes, this allowed model estimation on different levels of linearity to be tested.

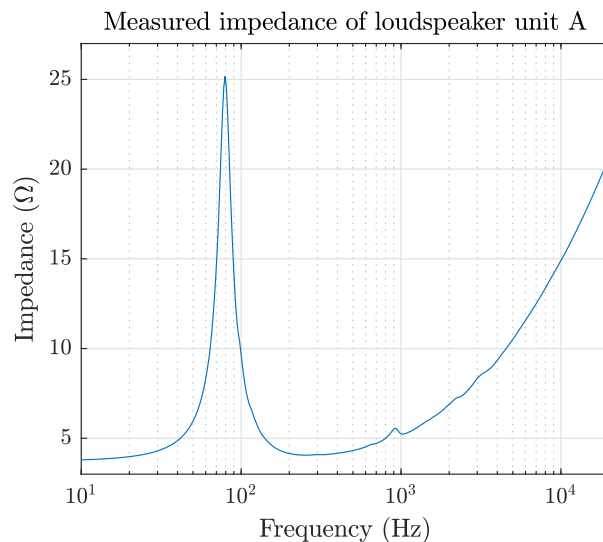Figure 3.1: Impedance bode plot of loudspeaker unit A measured with the Bode 100.

In order to verify that the system identification procedure is valid for regular use of a power amplifier, music was also used as an additional input excitation signal. In [5] it was shown that acoustic music had the most spread in frequency content, which is why this type of music was used for this thesis project as well.

3.1.3 Verification of measuring equipment

The measurements of the loudspeaker impedance was verified on loudspeaker unit A using the Omnicron Bode 100 system. The Bode 100 was connected to the loudspeaker unit and measured the impedance using a logarithmic frequency sweep from 10 Hz to 20 kHz.

3.2 Loudspeaker parameter identification

The modelling was primarily done using the System Identification Toolbox (SITB) in MATLAB. This toolbox contains a wide range of tools that can be used for the parameter estimation, in particular the grey-box model estimation. This allows a state space model such as the linearized electromechanical model of the loudspeaker with its related parameters to be estimated from collected data using optimization solvers.

For the identification of the linear small-signal parameters, the models used were five linear grey-box models in SITB, see Table 3.1. These models were chosen based on their wide use in previous studies. The parameters to identify here are the constant parameters specified earlier, M, R_{ms}, $R_e(T_0)$, $Bl(x = x_0)$, $L_e(x = x_0)$ and $C_{ms}(x = x_0)$, where x_0 is the operating point of the diaphragm.

The identification procedure was initiated using the SITB transfer function estimation method. This model structure can be seen in (2.5). Details on the parameters of each model structure can be seen in Table 3.1. The four other linear model structures used were a three state (cone displacement, cone velocity and current) state space model derived from (2.1)-(2.3) and the linearized state state space models from (2.6)-(2.8) with one, two and three LR-networks respectively.

Table 3.1: Parameters of the model structures in SITB.

Model structure	Parameters
Transfer function	M, R_e, $C_{ms}(x_0)$, $Bl(x_0)$, R_{ms}
State space (3 states)	M, R_e, $C_{ms}(x_0)$, $Bl(x_0)$, R_{ms}, $L_e(x_0)$
State space (4 states, LR-2)	M, R_e, $C_{ms}(x_0)$, $Bl(x_0)$, R_{ms}, $L_e(x_0)$, L_2, R_2
State space (5 states, LR-3)	M, R_e, $C_{ms}(x_0)$, $Bl(x_0)$, R_{ms}, $L_e(x_0)$, L_2, R_2, L_3, R_3
State space (6 states, LR-4)	M, R_e, $C_{ms}(x_0)$, $Bl(x_0)$, R_{ms}, $L_e(x_0)$, L_2, R_2, L_3, R_3, L_4, R_4
Nonlinear grey-box	M, R_e, $C_{ms}(x)$, $Bl(x)$, R_{ms}, $L_e(x)$, L_2, R_2

Initial values for all estimations were taken from parameter values of loudspeakers from other studies.

The model error metric chosen for comparison between the model structures was Normalized Root Mean Squared Error (NRMSE). This metric shows the error relative to the measured data. This allows model structures and different data set sizes to be compared.

Since the behaviour of the drift due to temperature increase in the linear parameters is unknown apart from the percentual increases found in [1] and [5], an approach was used to investigate the exact behaviour of the parameters with increasing voice coil temperature. By heating the voice coil with a DC power supply connected to the loudspeaker terminals, data was collected as the voice coil was cooling down. Noting the initial and final temperature of the voice coil during the entire measurement, Newtons law of cooling was used to establish the temperature at each time instant of the voltage/current measurement data. The data could thus be divided into temperature intervals, where the parameters could be estimated on the data of each interval.

3.3   Imposed defects

After conducting measurements on the functioning loudspeaker units, destructive measures was used to simulate a failure or irregular behaviour caused by overloading, aging, external factors etc. The two defects used in this thesis was chosen due to their frequent occurrence in audio installations, the severity of the failures and the practicability of imposing such defects.

In order to overheat loudspeaker unit A, a DC power supply was connected to the loudspeaker terminals. Through an opening in the dust cap of the loudspeaker, the temperature of the voice coil was monitored using a thermal camera.

The suspension failure was imposed by cutting a tear around one fourth (loudspeaker unit B) and one half (loudspeaker unit A, B, C) of the spider (see Figure 2.1).

4

Model estimation and fault detection simulation

In this chapter, the results of the model estimations on measured loudspeaker data is presented. These results include estimations using different input signals, model structures and loudspeaker defects. The chapter is rounded off with simulation results from proposed loudspeaker fault detection methods.

The loudspeaker samples used for data collection and the imposed defects of the units can be seen in Table 4.1.

Table 4.1: Loudspeaker units used for testing.

Loudspeaker unit	Diameter [mm]	Imposed defect
A	155	Overheated voice coil, suspension failure
B	370	Suspension failure
C	300	Suspension failure, validation

4.1 Model selection

The results of the model estimation and comparison using the model structures used in this thesis is presented in this section. The comparison starts with the low frequency five-parameter transfer function model and the model is then extended with additional parameters for modelling high frequency behaviour. The influence of different input signal levels on the model estimation performance can also be seen.

4.1.1 Model structures
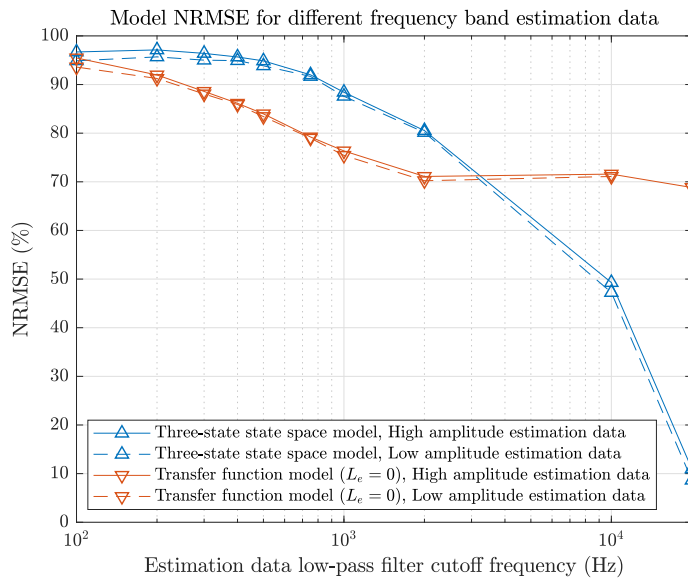
Figure 4.1: Model error for different frequency band estimation data, voice coil inductance in the model.

As is shown in Figure 4.1, the model error of the simple five-parameter transfer function model increased quickly with higher frequencies. Since all the parameters of this model are low frequency parameters, the combination of a lower frequency resolution around the resonance frequency and the estimation pulling the low-frequency parameters to model the higher frequency behaviour results in a steep decrease in NRMSE. Introducing the voice coil inductance into the model results in a better high and low frequency validity, possibly indicating that the inductance of the voice coil to some degree affects the impedance even at very low frequencies.

Introducing a LR-network to the model allows it to capture the high frequency behaviour due to eddy currents in the pole structure. This is illustrated in Figure 4.2. This makes the model error more or less constant for frequencies up to 1 kHz by granting the model more flexibility in the higher frequency range.
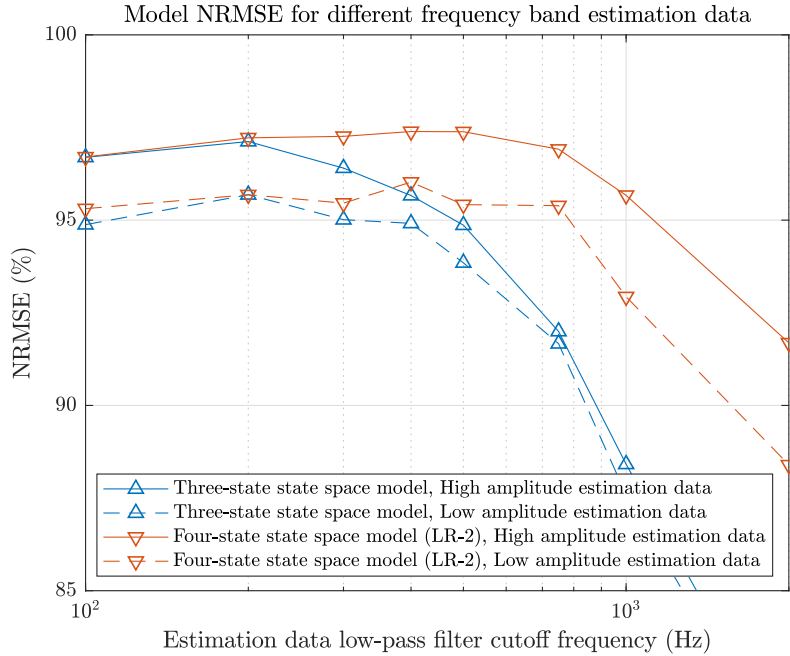

Figure 4.2: Model error for different frequency band estimation, voice coil inductance and eddy currents in the model.
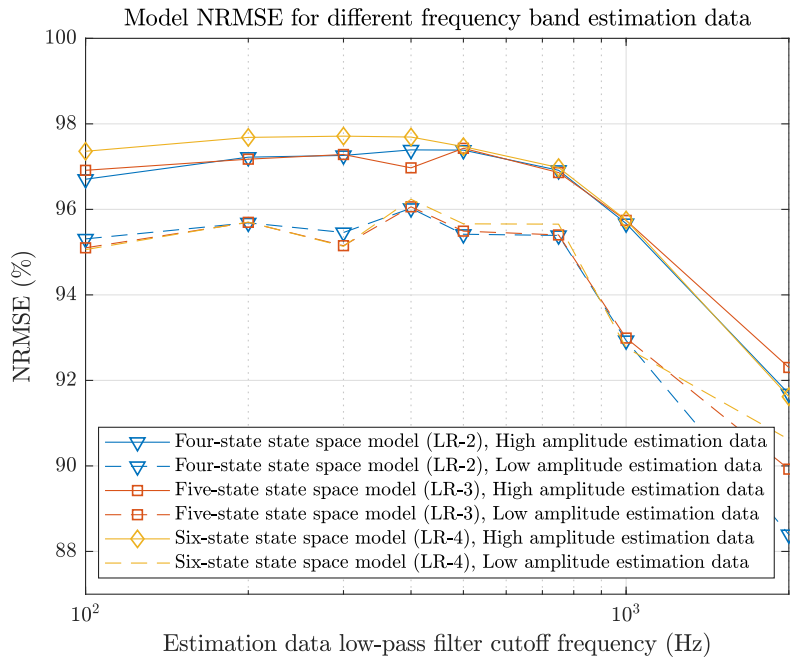

Figure 4.3: Model error for different frequency band estimation data, one, two and three cascaded LR-networks in the model.

By cascading several LR-networks as Figure 4.3 shows, the model can be made even more flexible for high frequencies. However, the model error was in fact not reduced significantly with the addition of one or two more LR-networks in series, possibly indicating that high frequencies in the data is already sufficiently captured by the LR-2 addition to the model.
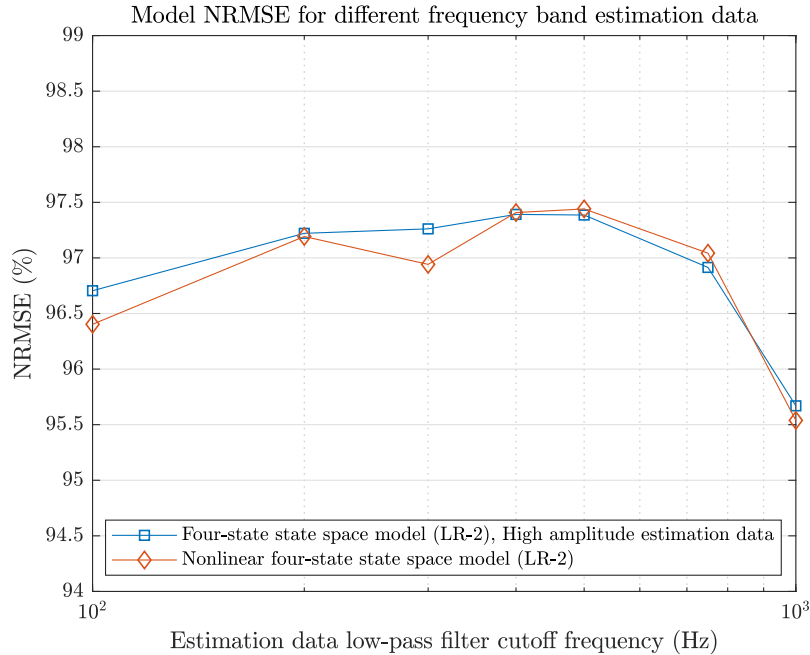
Figure 4.4: Model error for different frequency band estimation data, nonlinearities in the LR-2 model.

The nonlinear model also includes one LR-network as in the LR-2 model, but uses a Gaussian sum as an approximation of the nonlinearity in the suspension compliance and the force factor. The voice coil inductance is modelled using a sigmoid function. Performance-wise, the nonlinear model does not show any advantage over the linear LR-2 model for this particular estimation data set, see Figure 4.4. This is possibly due to the input signal driving the loudspeaker in the mostly linear region of operation. Furthermore, the nonlinear model requires the estimation of seven additional parameters, possibly introducing numerical issues in the solver.

4.1.2 Final model choice

Since a majority of the Thiele/Small-parameters are related to the resonance peak of the loudspeaker and considering the similarities of the moving coil loudspeaker with a low frequency second degree mechanical system, the three state state space model (see (2.6-2.7)) was chosen for the parameter estimation in this study. This model includes the effect of the voice coil inductance for low frequencies, while not adding additional high frequency parameters that can affect the estimation of the parameters of the mechanical system.

4.2   Input signal choice

The result of investing the two different input signal parameters, amplitude and frequency band is presented in this section.

4.2.1   Amplitude

What was seen in Figures 4.1-4.3 was that high amplitude input signals (1 V) resulted in a lower NRMSE for all the linear model structures. This is possibly due to the high amplitude input signal not driving the loudspeaker enough for it to leave the "mostly linear" region of operation. This proposition is supported by the power spectral density plots of the input and output signal shown in Figure 4.5(a), where the output signal (current) seemingly contains no harmonic overtones of the input signal. The high amplitude input signal is thus still suitable for linear model estimation and results in data with a higher signal-to-noise ration (SNR) than in the lower input signal data.
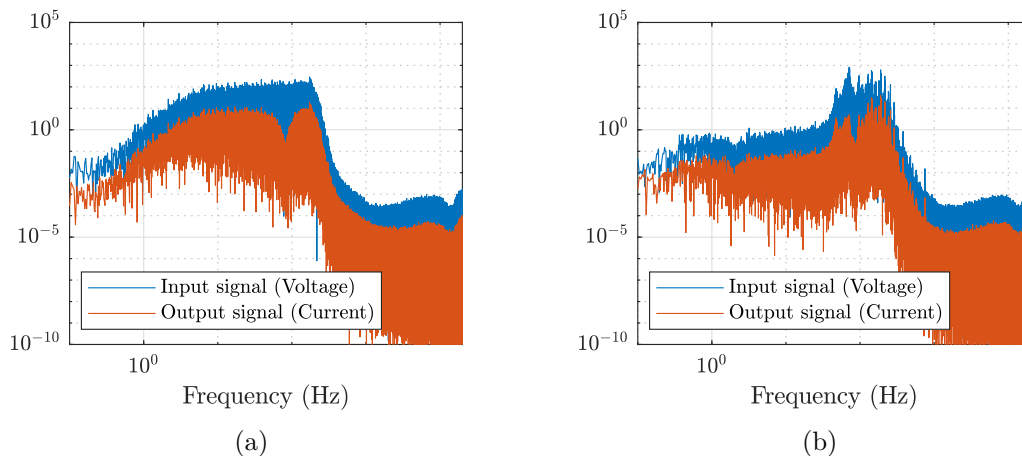
Figure 4.5: Power spectral density of voltage and current measurements on loudspeaker unit A using a low pass filtered white Gaussian noise signal with cutoff frequency 200 Hz, (a), compared to the power spectral density of using a music signal filtered with the same filter, (b).

4.2.2   Frequency band of input signal

The relationship between model error and input frequency band is consistent with the frequency dependence of the parameters discussed in Section 2.1.3, as Figures 4.1 - 4.4 show. Using an input signal filtered with a low pass cutoff frequency of 200 Hz, the model error on similar validation data is the lowest for most of the models as the frequency resolution around the resonance frequency is high for such a signal. Considering the numerical issues appearing during estimation on high frequency estimation data and the fact that most of the parameters are identifiable from the resonance peak, the input signal was chosen to the frequency band 0 - 200 Hz.

4.2.3   Music as input signal

The estimated parameters of loudspeaker unit A using low-pass filtered music as input signal together with the parameters estimated using filtered WGN can be seen in Table 4.2.

Table 4.2: Estimated Thiele/Small parameters of loudspeaker unit A using low-pass filtered music as an input signal.

Input signal	$\hat{R}_e$ [Ω]	$\hat{f}_n$ [Hz]	$\hat{Q}_{es}$	$\hat{Bl}$ [Tm]	$\hat{L}_e$ [mH]
Music	3.70	79.74	1.27	5.45	0.42
White Gaussian noise	3.68	79.60	1.24	5.60	0.45

Looking at Figure 4.5(b), where an acoustic music track was filtered using a low-pass filter with cutoff frequency of 200 Hz, the frequency content of such a signal can be seen. Although the frequencies of this signal below 40 Hz are highly attenuated compared to the filtered WGN signal in Figure 4.5(a), the energy below 1 Hz is higher for this signal. This results in the accurate voice coil resistance parameter estimation seen in Table 4.2, where the resistance of loudspeaker unit was measured to 3,70 Ω using the Bode 100. This use of music as an input signal also results in a resonance frequency estimation closer to the measured frequency using the Bode 100, 80.09 Hz.

4.3   Temperature parameter drift

The Thiele/Small parameters estimated on data at different voice coil temperatures can be seen in Figure 4.6.
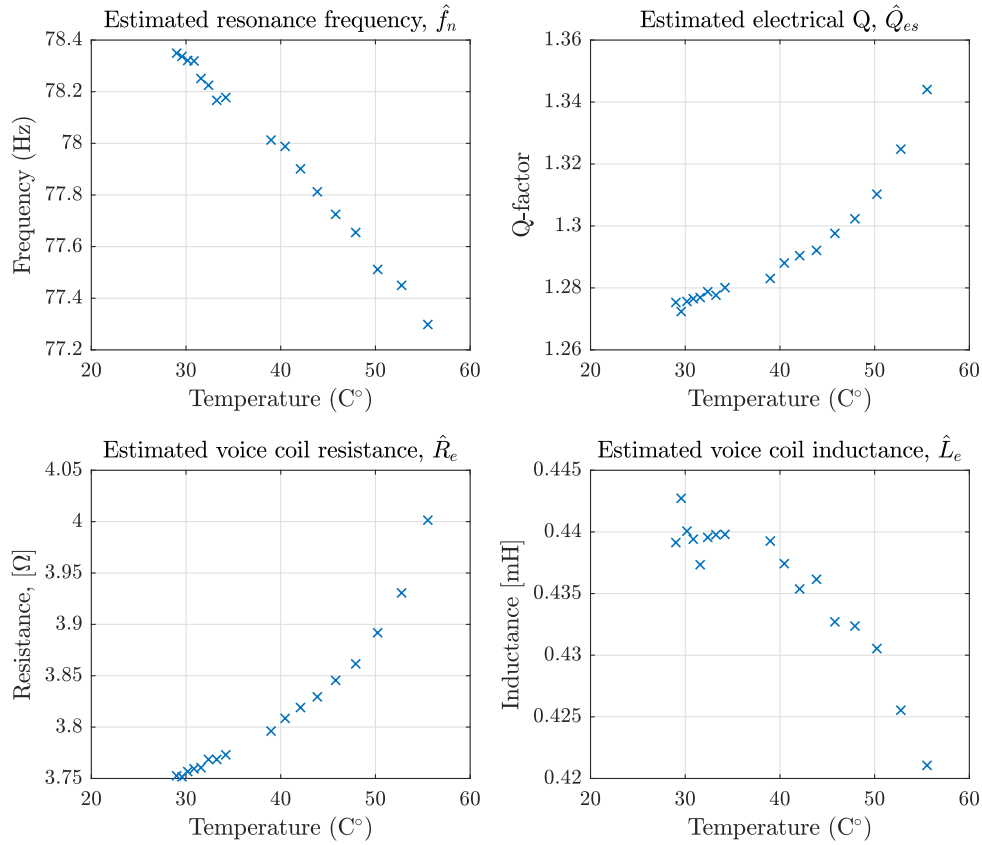
Figure 4.6: Loudspeaker parameter change due to increasing voice coil temperature. Three outlier data points due to measurement errors between 35 °C and 40 °C removed from plots.

As these figures illustrate, all estimated parameters seem to be affected by a change in temperature in the voice coil. Percentual changes in the parameters due to a 30 °C temperature increase can be seen in Table 4.3 and the results compared to a previous study can be seen in Table 4.4.

Table 4.3: Thiele/Small physical parameter drift due to a 30 °C temperature increase.

Parameter	23 °C to 53 °C parameter drift (Measurement, loudspeaker unit A)
R_e	6.8 %
f_n	-2.7 %
Q_{es}	7.0 %
Bl	-3.6 %
L_e	-6.2 %

Table 4.4: Thiele/Small parameter drift due to a 30 °C temperature increase. Measured parameter drift compared with parameter drift found in [1].

Parameter	20 °C to 50 °C parameter drift (Krump, 1997)	23 °C to 53 °C parameter drift (Measurement, loudspeaker unit A)
R_e	11 %	6 %
Bl	-6 %	-4 %
M	-3 %	-4 %
C_{ms}	21 %	10 %
R_{ms}	-20 %	-9 %

Although the results found in this study presented in Table 4.4 show behaviour similar to that found in [1], it also shows that there is a significant difference in the temperature dependence of the parameters between different loudspeaker units. This can be deduced as some of the parameters of the car loudspeaker in [1] drift twice as much as the parameters of loudspeaker unit A during a similar temperature increase.

4.4 Parameter variation due to failure modes

The percentual change in the estimated Thiele/Small parameters due to the imposed failure modes can be seen in Table 4.5. These parameters are estimated using the chosen three state state space model.

Table 4.5: Three state state space model parameter deviation due to imposed failure modes. Parameter deviation due to the second defect in the overheated loudspeaker unit is given relative the overheated loudspeaker state.

Loudspeaker defect	$\Delta \hat{R}_e$ [%]	$\Delta \hat{f}_n$ [%]	$\Delta \hat{Q}_{es}$ [%]	$\Delta \hat{Bl}$ [%]	$\Delta \hat{L}_e$ [%]
Overheating, unit A	3.20	-1.31	2.73	-10.58	-3.76
Overheating and suspension tearing, unit A	0.18	-6.63	-11.14	13.82	8.54
Suspension tearing (1/4 of spider), unit B	0.16	-1.03	-0.01	-3.69	-0.07
Suspension tearing (1/2 of spider), unit B	0.34	-1.17	0.19	-8.23	-0.30
Suspension tearing (1/2 of spider), unit C	-6.62	-16.70	-36.87	16.22	-18.07

Table 4.6: Deviation in resonance frequency and damping ratio calculated from denominator coefficients of OE model due to imposed failure modes. Parameter deviation due to the second defect in the overheated loudspeaker unit is given relative the overheated loudspeaker state.

Loudspeaker defect	$\Delta \hat{f}_n$ [%]	$\Delta \hat{\zeta}$ [%]
Overheating, unit A	-3.45	14.35
Overheating and suspension tearing, unit A	-5.11	-6.97
Suspension tearing (1/4 of spider), unit B	-3.20	11.50
Suspension tearing (1/2 of spider), unit B	-3.41	11.45
Suspension tearing (1/2 of spider), unit C	5.65	-1.35

The variation in estimated resonance frequency deviation of Table 4.5 compared to Table 4.6 is due to the continuous state space model having three poles, while the OE model used to estimate the system only has two.

Parameter deviations in the calculated resonance frequency and damping ratio of the estimated OE model can be seen in Table 4.6. The resonance frequency and damping ratio are calculated from the denominator coefficients of the OE model, a_1 and a_2, as described in Section 2.2.2.

As loudspeaker unit A was overheated, the most significant parameter deviation was the reduction in force factor. As the glue keeping the turns of wire of the voice coil closely together starts to soften, the coil loosens from the former making the coil less compact in the gap, thus reducing the force that the magnetic field generates as current passes through the coil. This can also be seen in the reduction of the voice coil inductance parameter. Calculating the total damping ratio of the driver using the denominator coefficients of the digital filter presented in Table 4.6, a large deviation in mechanical damping is observable. This is probably due to the mechanical friction in the gap that occurs when the voice coil is slightly unwound from the former.

As loudspeaker unit A was exposed to an additional defect, as Table 4.5 illustrates, significant changes was observed in all parameters except for the voice coil resistance, which is expected. The increase in suspension compliance due to the suspension tearing leads to a lower resonance frequency and the increase in force factor leads to a reduction in electrical Q factor. The increase in voice coil inductance is a bit more questionable, as this indicates that the permeability of the surrounding of the voice coil would change. This could be explained by a possible voice coil offset due to the less stiff suspension, positioning the coil closer to the magnet. This is provided that the voice coil is overhung, i.e. extends out of the magnetic field gap. This would then also explain the increase in force factor, having more turns of wire inside the loudspeaker magnet structure but with a less linear behaviour due to the less homogeneous magnetic field. The results of Table 4.6 and Figure 4.15 are both compliant with these results.

The suspension failure of loudspeaker unit B caused a decrease in force factor and a small decrease in resonance frequency. The electrical Q factor however remains unchanged, indicating a decrease in the moving mass parameter. Observing the increase in the total damping ratio estimated using a recursive algorithm in Table 4.6 and comparing the results with (2.14), this is a reasonable assumption.

As previously mentioned, loudspeaker unit C exhibited similar parameter deviations to loudspeaker unit A as a consequence of suspension breakdown. As Table 4.5 shows, both units experience a significant decrease on resonance frequency and electrical Q factor as well as a large increase in force factor. Since the estimation of the OE model seen in Table 4.6 failed to converge to the correct minima, the parameter deviations in this table for this loudspeaker unit are erroneous and should be disregarded.

4.5 Fault detection implementation

Using the theoretical results from Section 4.4, two approaches for online fault detection are proposed in this section. One using a system identification based recursive model estimation approach and one lower complexity filter based approach.

4.5.1 Recursive model estimation

As the poles of the simplified second order transfer function model can be used to calculate the damping and natural frequency, the poles of the digital filter equivalent can be used to calculate these parameters as described in Section 2.2.2. In Figures 4.7-4.12 a recursive OE model using a Kalman filter algorithm in Simulink is used to estimate the poles of the system as the data of the fault free loudspeaker sample is replaced with data from the loudspeaker sample exhibiting defective behaviour. The digital filter coefficients of this estimation are then used to calculate the resonance frequency and damping ratio.
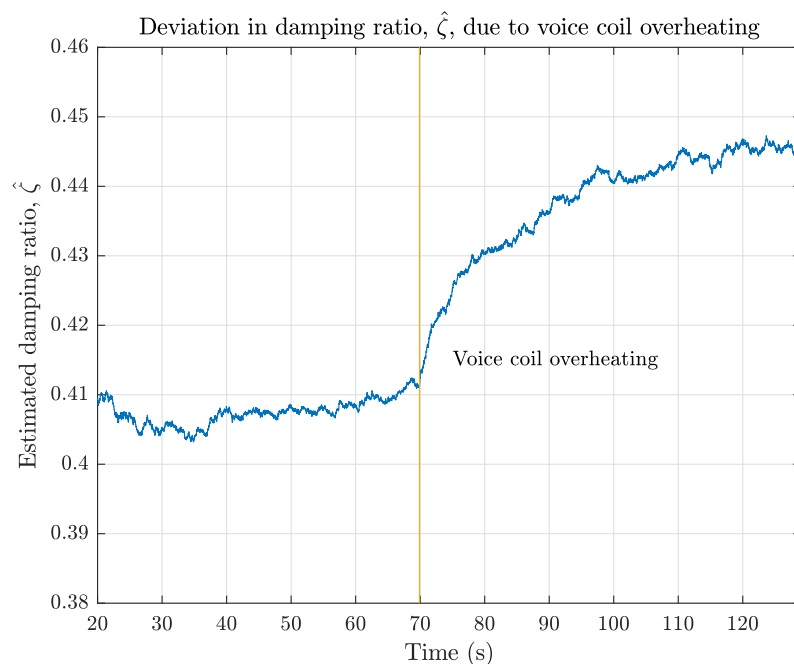

Figure 4.7: Recursive model damping ratio estimation deviation due to voice coil overheating, loudspeaker unit A.
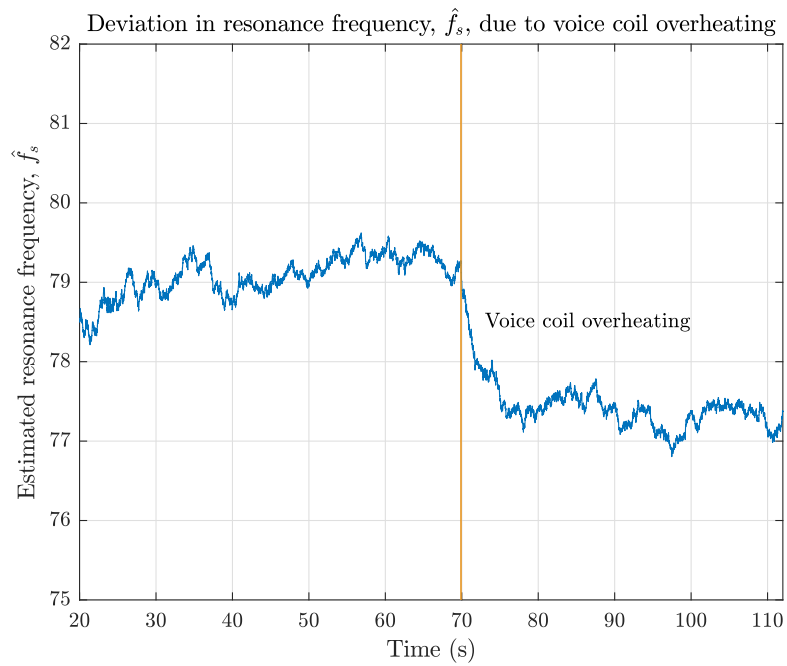
Figure 4.8: Recursive model resonance frequency estimation deviation due to voice coil overheating, loudspeaker unit A.

Figure 4.9: Recursive model damping ratio estimation deviation due to suspension failure, loudspeaker unit B.

Figure 4.10: Recursive model resonance frequency estimation deviation due to suspension failure, loudspeaker unit B.

Figure 4.11: Recursive model damping ratio estimation deviation due to suspension failure, loudspeaker unit C.

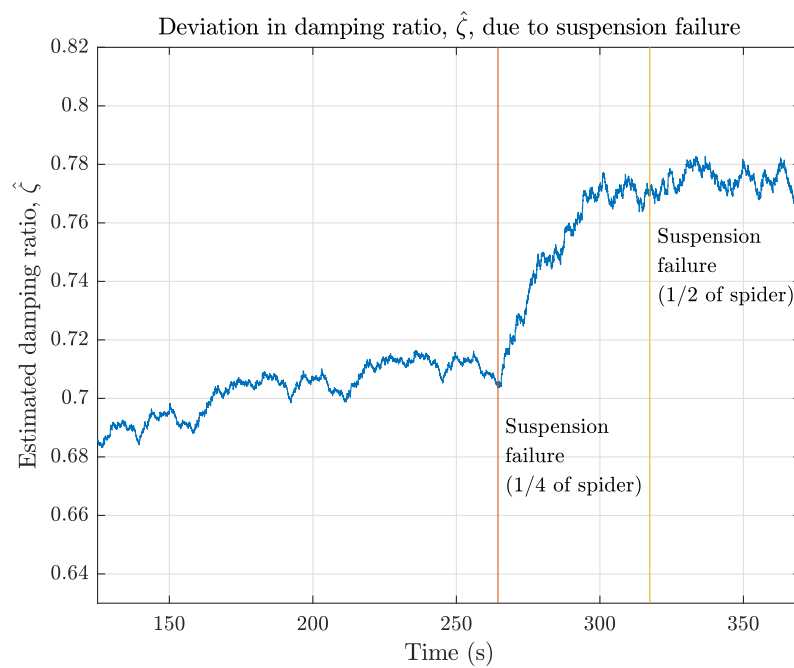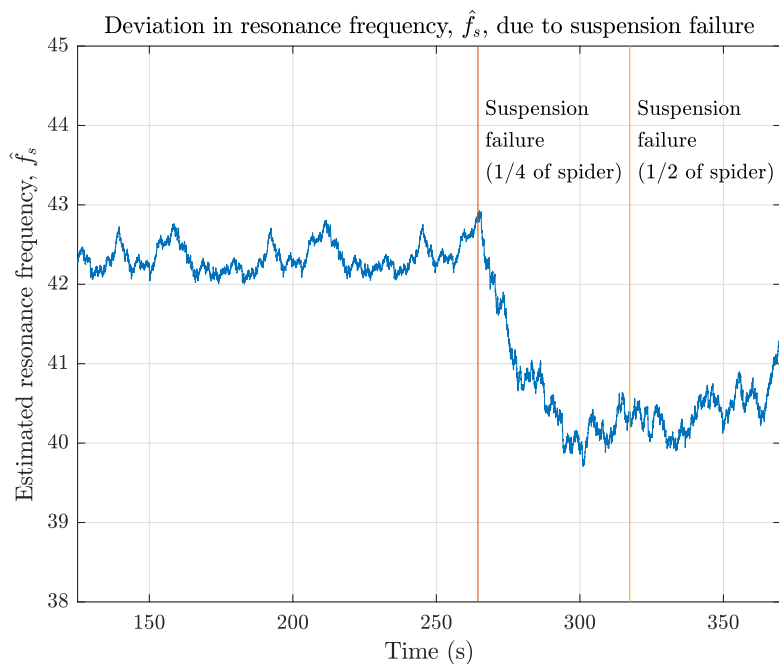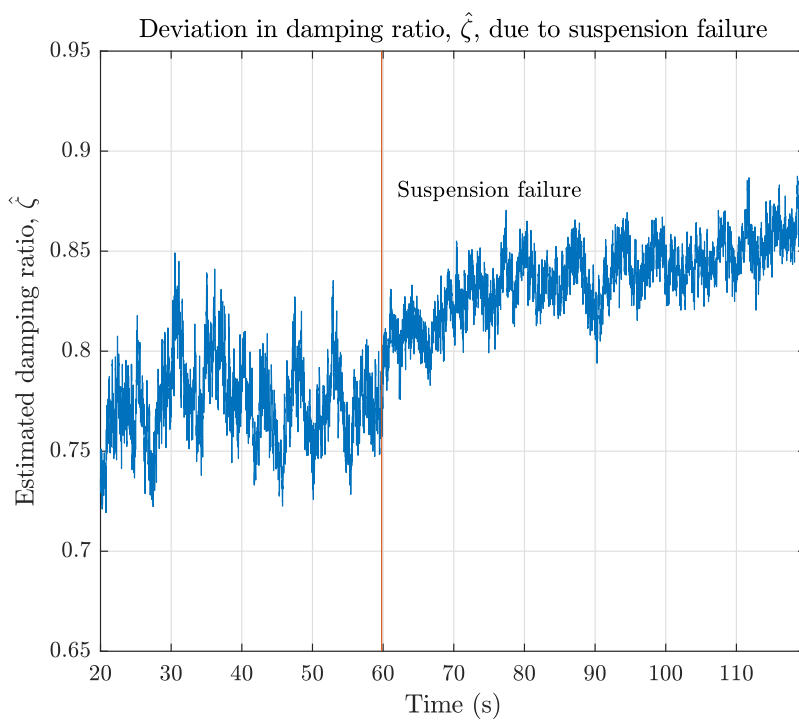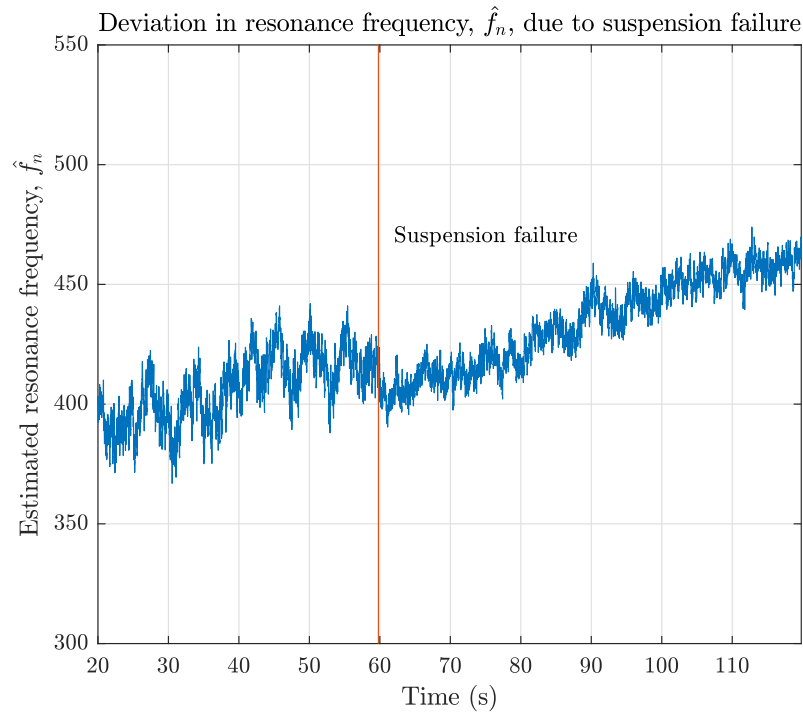Figure 4.12: Recursive model resonance frequency estimation deviation due to suspension failure, loudspeaker unit C.

As can be seen in Figures 4.7-4.10, the recursive model estimation results are compliant with the offline estimated deviations seen in Table 4.6. While the system suffers from slow convergence of the parameters, the deviations are highly significant and the change could easily be detected by software in a power amplifier.

Figures 4.11-4.12 shows how the loudspeaker defect causes a convergence from one erroneous local minima to another (resonance frequency of loudspeaker unit C in reality around 50 Hz). The results seen in Figures 4.11-4.12, following the skewed results from this unit seen in Table 4.6, should thus also be mostly disregarded. This will be discussed further in Chapter 5.

4.5.2 Impedance estimation using peak filtering

The change in total driver Q factor can also be detected by filtering the voltage and current measurements and calculating the impedance. As the total Q factor is related to the bandwidth of the resonance peak, as discussed in Section 2.1.3, the impedance at the frequencies close to the resonance frequency will increase or decrease depending on the value of this parameter. A narrow resonance peak will have a low impedance at neighbouring frequencies while a broad resonance peak will have high. Using one or more peak filters, this impedance at these frequencies can easily be calculated. In Figure 4.13 the measured data from the fault-free loudspeaker unit A is replaced at $t = 47$ s. with the measurements from the unit after overheating it, simulating a breakdown.
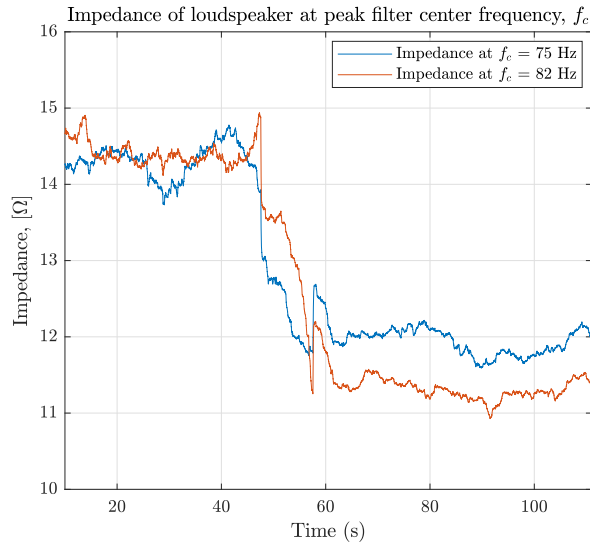
Figure 4.13: Impedance measurements using peak filters on both sides of the driver resonance peak as voice coil overheating occurs, loudspeaker unit A.

Using two peak filters at center frequency $f_c = 75$ Hz. and $f_c = 82$ Hz. (resonance frequency of fault-free driver $f_n = 80$ Hz.), the impedance was calculated from the RMS values of the voltage and current using a sliding windows of 10 seconds. As Figure 4.13 illustrates, the impedance on both sides of the resonance peak is reduced significantly as the defect is introduced, since the overheated loudspeaker unit has a higher Q factor i.e. more narrow resonance peak.

Figure 4.14: Impedance measurements using peak filters on both sides of the driver resonance peak as suspension failure occurs at different input signal levels, loudspeaker unit C.

Using the same approach on the data measured from loudspeaker unit C, exhibiting an imposed suspension breakdown defect, the results seen in Figure 4.14 was observed. Contrary to the overheating defect, the resonance peak of loudspeaker unit C widened as the defect was imposed. This resulted in a higher impedance at the peak filter frequencies neighbouring the resonance frequency and thus a lower Q factor.

Figure 4.15: Impedance measurements using peak filters on both sides of the driver resonance peak as voice coil overheating and suspension breakdown occurs, loudspeaker unit A.

Using loudspeaker unit A, an attempt to replicate these results by imposing a similar suspension failure defect onto the already overheated sample was made. The results can be seen in Figure 4.15 and are compliant with the behaviour seen in loudspeaker unit C. The large increase in impedance at $f_c = 75$ Hz. compared to the increase in $f_c = 84$ Hz. indicates a decrease in resonance frequency, moving the high impedance of the resonance peak into the 3 dB bandwidth of the peak filter.
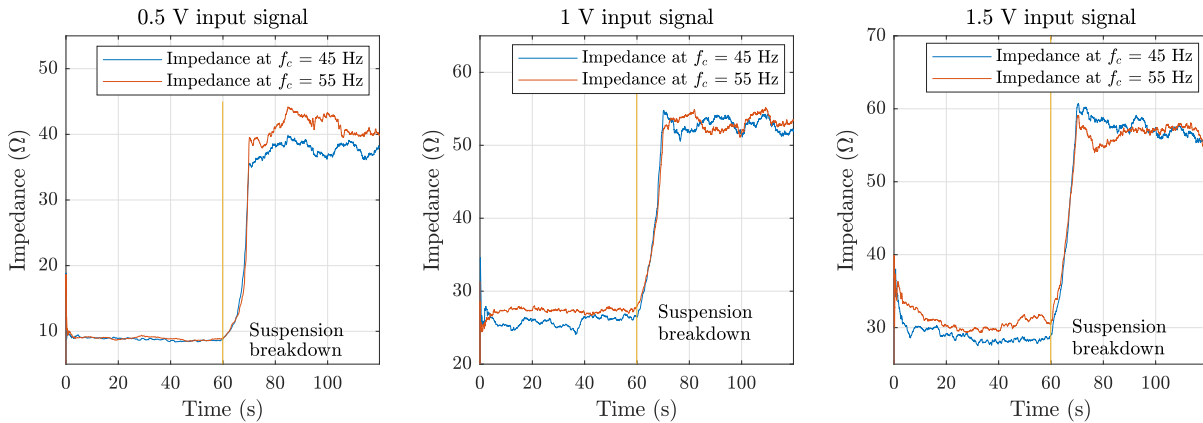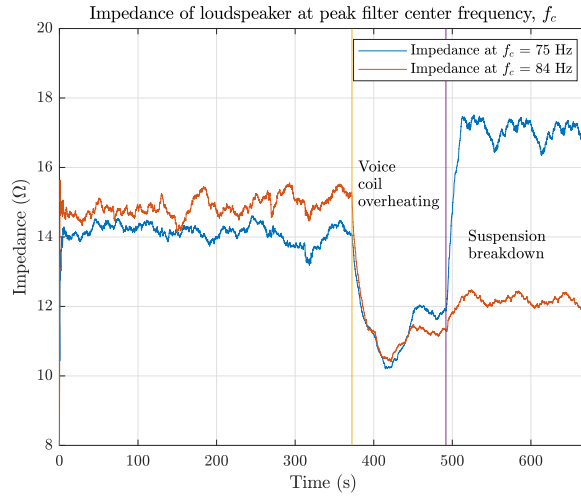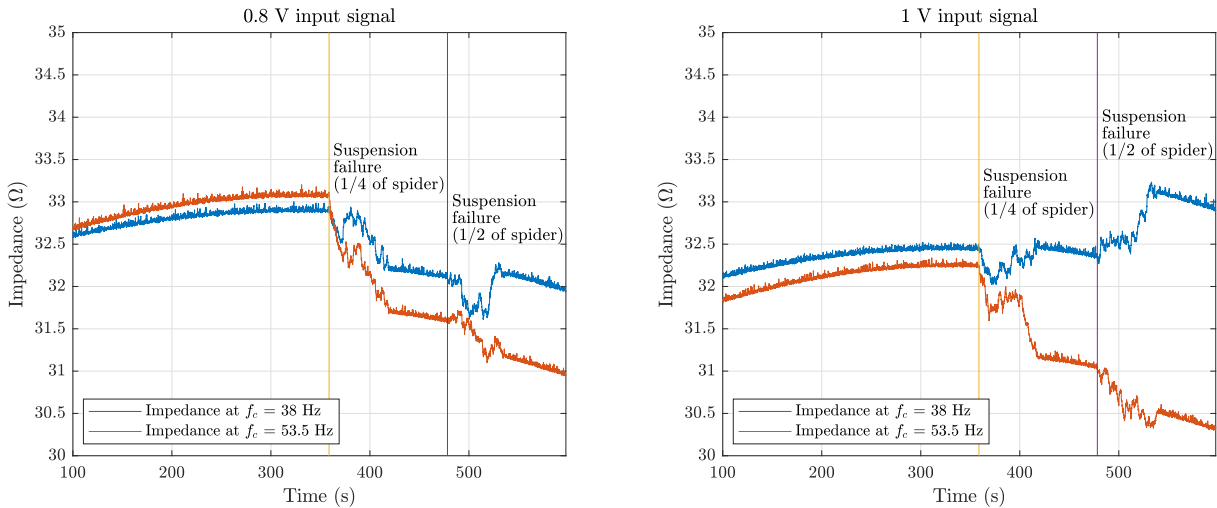

Figure 4.16: Impedance measurements using peak filters on both sides of the driver resonance peak as suspension failure occurs at different input signal levels, loudspeaker unit B.

Finally, the peak filter approach was used on loudspeaker unit B, also exhibiting a suspension failure. Figure 4.16 shows the impedance above and below the resonance frequency during the imposed breakdown scenario. Using a lower amplitude input signal (0.8 V), the resonance peak becomes more narrow, while when using a higher amplitude input signal (1 V), the resonance peak becomes more narrow and the resonance frequency is lowered. The reduction in resonance frequency using the high

amplitude input signal is deducted using the same reasoning as with the resonance frequency reduction of loudspeaker unit A. A reasonable assumption aiding the explanation of these results is that the tearing in the suspension, securing the voice coil in its gap, caused some voice coil rubbing in the loudspeaker, i.e. introducing mechanical friction causing the system to be more damped in its oscillations. The contradicting results where loudspeaker unit A and C became *less* damped as the suspension broke down can thus be explained.

Deviations in impedance due to different input signal levels can be observed in Figure 4.14 as well as in Figure 4.16. This could either indicate the presence of nonlinear behaviour or, more likely, measurement errors from the equipment. This will be discussed further in Chapter 5.

5

Discussion

5.1 Implementation aspects

The implementation of an online fault detection system can be divided into two problems; accounting for parameter drift due to temperature increase and the detection of parameter change due to a defect in the loudspeaker.

5.1.1 Compensation of temperature increase

The importance of accounting for parameter drift due to increasing temperature in the voice coil of the loudspeaker becomes obvious by looking at Table 4.3 and Table 4.5. The increase in electrical Q factor due to an overheated voice coil can for instance be completely overshadowed by a temperature increase of 30 °C or more during regular operation of the loudspeaker. This issue can be resolved in a number of ways. One possible solution is to use the resistance of the voice coil as a temperature indicator. Using linear or polynomial models for each parameter as a function of temperature, the change due to temperature increase could be compensated for, leaving only the parameter change due to a defect to be detected. While this is a completely feasible solution to implement, the robustness of such a system can be questioned; as can be seen in Table 4.4, the parameter drift due to temperature increase can differ a lot from speaker to speaker (drift in [1] measured on a car loudspeaker).

A much simpler solution to the problem is to continuously measure the voice coil DC-resistance and to only activate the fault detection system when the measured resistance increase is within a set interval, for instance 0 - 2 % corresponding to a temperature increase interval of approximately 0 - 15 °C. Given that measurements of voltage and current are available in the power amplifier unit, the DC-resistance can easily be tracked by low pass filtering the measurements and dividing the RMS values of the voltage by the RMS of the current, both calculated on a sliding window of samples.

5.1.2 Compensation of nonlinear behaviour

While the amplitude level of the input signal during the measurements in this study was controlled to only drive the loudspeaker within the "mostly linear" region of operation, this can of course not be guaranteed during normal use of a power amplifier. As seen in [2], the parameters of the linear LR-2 model can change as much as 50 %

for very large voice coil excursions (8.57 mm.). This resulted in a change of resonance frequency by 13 %. As a nonlinear loudspeaker model proved to be unfeasible to use for online parameter estimation using only current and voltage as measurements, an easy circumvention method would be to limit the online parameter estimation algorithm to only be active for certain voltage RMS intervals.

5.1.3   Classification of defects

As the results of this study has shown, the most significant and detectable parameter deviations in loudspeakers due to overheating and suspension failure is in the resonance frequency and damping factor. While a defect could be classified based on the nature of the parameter deviation in theory, it poses a bigger challenge in practice. Detecting a decrease in the damping factor of a loudspeaker would, based on the results seen in this study, indicate a loosening of the suspension or other parts of the loudspeaker, allowing the voice coil to move more freely. If the voice coil is allowed too much freedom however, it is likely that it will collide with other parts of the loudspeaker. This especially considering that the space in the voice coil gap often times is measured by fractions of millimeters. Adding such mechanical friction instead causes the damping factor to increase, making the suspension failure indistinguishable from a defect due to overheating of the voice coil.

As seen in Chapter 4, there are inconsistencies in the measured data when it comes to different amplitude levels of the input signal. In Figures 4.14 and 4.16 the measured impedance varies with the input signal level. Unexpected deviations in voice coil DC-resistance can also be seen in Table 4.5. Depending on the thermal characteristics of the voice coil of a particular loudspeaker unit, the DC-resistance could vary from data set to data set if the excitation during data collection is enough to heat the voice coil by several degrees. This could explain the aforementioned deviations in the results.

The use of the voice coil inductance as a parameter in the model provides a lower model error, but considering the low frequency excitation of the loudspeakers in this thesis, the reliability of the estimation of such a high frequency parameter must be questioned. The significant changes in this parameter due to various failure states as seen in Table 4.5 substantiate this presumption. For the inductance of the voice coil to change significantly without any alterations to its shape or density of winding, a very large voice coil offset would be required, changing the permeability of its surroundings. Removing this parameter from the model and lowering the cutoff frequency of the input signal low pass filter could possibly result in less bias of the remaining low frequency parameters.

5.2   Future work

One of the major drawbacks of the chosen methods in this thesis project was the lack of unique solutions to the optimization problem of minimizing the model error. Apart from having to redo some work upon realization, this leaves a gap in the result where the parameter deviation in some Thiele/Small-parameters is missing, for example the mechanical resistance R_{ms}, moving mass M and suspension compliance C_{ms}. Reliable measurements of the loudspeaker diaphragm position would allow all Thiele/Small parameters, including nonlinear terms, to be identified. While this holds academic value, this measurement is unavailable during consumer use of a power amplifier and was therefore of less interest in this thesis project. For loudspeaker testing and diagnosis, this is an interesting topic and could be investigated in future work.

One effect of the lack of unique solutions and convergence to local minima not related to the true physical parameter values can be seen in Figures 4.11-4.12. The results in simulation are not compliant with the results seen in Table 4.6 and even those values for this loudspeaker unit should be considered fairly unreliable considering the large model error seen during estimation (~ 80 %). Given the physical dimensions of loudspeaker unit C, the resonance frequency of the driver is around 50 Hz. During estimations using the measurements on this unit however, the solver converged to local minima ranging from 200 Hz to 700 Hz, regardless of the initial condition provided. This creates a problem with the physical parameter system identification approach for the fault detection implementation. Nevertheless, as Figures 4.11-4.12 and to some extent Table 4.6 show, introducing data from the defective loudspeaker to the algorithm does cause a significant parameter deviation, albeit in parameters perhaps more regarded as "black-box parameters" for this loudspeaker unit. Further work could investigate the implementation of continuous model online batch-processing, i.e. recording voltage and current in blocks and performing "offline" parameter estimations based on the Thiele/Small model on each block, to minimize this risk.

A limitation with the results found during this thesis project is that the measurements conducted and model structures used were performed on one single woofer, without enclosure. In reality a power amplifier is often connected to multiple loudspeakers and cross-over networks, mounted in closed or vented enclosure. This highly affects the impedance of the load, and the model structure would have to be extended to include several resonance peaks due to tweeters and the resonance of the enclosure. As the main results of this thesis project is that common loudspeaker failures can be detected by the width of the resonance peak and the shift in resonance frequency, the detection of a defect in an audio system consisting of several loudspeakers might not even require the use of models, as shown possible by the peak filter approach in Section 4.5.2.

Furthermore, a real implementation of a fault detection and diagnostisation system using the results of this study is also relevant for future work. This investigation

could include the development of a robust algorithm that ensures that the detected parameter deviation is due to an actual defect and not an increase in voice coil temperature, nonlinear behaviour of the driver or changes in the excitation signal, as discussed previously in this section.

6
Conclusion

The results of this study has shown that the parameter deviation due to common failure modes loudspeaker is significant and detectable using system identification methods. As the moving coil loudspeaker in simplicity can be seen as a mechanical spring-damper system, any defective behaviour causing the voice coil to move differently appears in the pole placement of its linearized transfer function. Implementing a system in a power amplifier for detecting these changes will remove the need for the use of pilot tones, alert the user when a significant deviation from function is detected and thus improve the reliability in safety critical applications of the power amplifier. The wished outcome of the project is therefore reached.

As a result of the finding in this study, the choice of model structure for the loudspeaker impedance for the purpose of identifying loudspeaker faults does not seem to matter as much as previously suspected. While it was seen that the higher order models such as the LR-2 and its extensions resulted in a lower model error, the significance of a good model is probably more important for control purposes. A linearized low frequency grey-box model or a second order polynomial black-box model proved to be sufficient for the purpose of identifying changes in the resonance frequency and damping ratio of the driver, thus able to detect all the presented loudspeaker failure modes of this thesis.

For the failure modes investigated in this thesis project, small signal models were sufficient for the purpose of identifying defective behaviour in loudspeaker units. This could however aid the implementation of a fault detecting system, circumventing the problem of drift in the linear parameters due to nonlinear behaviour (see Section 5.1.2).

As a summary of the results of this thesis project:

- The LR-2 model and its extensions including additional LR-networks captures most of the dynamics of the system in terms of minimizing the model error over the full frequency range compared to the other investigated model structures of this thesis.

- Large signal/nonlinear models are not required for the detection of the loudspeaker failure modes investigated in this study.

- Black-box models can be used for the detection of the loudspeaker failure

modes investigated in this study, provided that the number of poles correspond to the number of poles of the true system.

- Changes in damping ratio ζ and resonance frequency f_n can indicate deviation from intended function or failure in a loudspeaker.

- These parameters can be identified using solely voltage, frequency and current measurements.

- Music as an input signal is feasible for the system identification and estimation of loudspeaker parameters, provided that the frequency spread of the music around the resonance frequency of the driver is even.

Bibliography

[1] G. Krump. "Zur Temperaturabhängigkeit von Lautsprecherparametern," presented at DAGA-97, Kiel, Germany, 1997.

[2] W. Klippel, U. Seidel. "Fast and Accurate Measurement of Linear Transducer Parameters." Internet: https://www.klippel.de/fileadmin/klippel/Files/Know_How/Literature/Papers/Fast_and_Accurate_Linear_Parameter_Measurement_01.pdf, [Apr. 25, 2018].

[3] W. Klippel, S. Irrgang, U. Seidel. "Loudspeaker Testing at the Production Line." Internet: https://www.klippel.de/fileadmin/klippel/Files/Know_How/Literature/Papers/Loudspeaker_Testing_at_the_production_line_06.pdf, [Mar. 6, 2018].

[4] W.J.N. Turner, A. Staino, B. Basu. (June, 2017). "Residential HVAC fault detection using a system identification approach". *Energy and Buildings.* [Online]. Vol. 151. Avaliable: https://doi.org/10.1016/j.enbuild.2017.06.008 [Jan. 26, 2018]

[5] B. Rohde Pedersen, "Error correction of loudspeakers: a study of loudspeaker design supported by digital signal processing," Ph. D. dissertation, Dept. of Software, Medialogy and Electronics., Esbjerg Tekniske Institut. Aalborg University, Esbjerg, Denmark, 2008.

[6] A. Bright, "Active Control of Loudspeakers: An Investigation of Practical Applications," Ph. D. dissertation, Dept. of Acoustic Technology, Technical University of Denmark, Lyngby, Denmark, 2002.

[7] D. Jakobsson, M. Larsson. "Modelling and Compensation of Nonlinear Loudspeaker." Master's thesis, Chalmers University of Technology, Sweden, 2010.

[8] V. Dickason. *Loudspeaker Design Cookbook*, 7th edition. Chase City, VA: KCK Media Corp. 2006, pp. 3.

[9] V. Dickason. *Loudspeaker Design Cookbook*, 7th edition. Chase City, VA: KCK Media Corp. 2006, pp. 4-5.

[10] A.N. Thiele. "Loudspeakers in vented boxes, parts i and ii". *Journal of Audio Engineering Society*, Vol. 19, pp. 382-293, 471-483, May 1, 1971.

[11] M. Dodd, W. Klippel, J. Oclee-Brown. "Voice Coil Impedance as a Function of Frequency and Displacement." Internet: https://www.klippel.de/fileadmin/klippel/Files/Know_How/Literature/Papers/Voice_Coil_%20Impedance_04.pdf, [Feb. 23, 2018].

[12] Svee. "Cross-section of a full-range loudspeaker driver using a whizzer cone design." Internet: https://en.wikipedia.org/wiki/File:FullRangeSpk.svg, 23 Oct. 2007, [7 Mar. 2018].

[13] M. R. Bai, C. Huang. "Expert diagnostic system for moving-coil loudspeakers using nonlinear modeling." *The Journal of the Acoustical Society of America*, Vol. 125, pp. 819-830, Feb. 2009.

[14] W. Klippel. "Loudspeaker Nonlinearities - Causes, Parameters, Symptoms." Internet: https://www.klippel.de/fileadmin/_migrated/content_uploads/ Loudspeaker_Nonlinearities%E2%80%93Causes_Parameters_Symptoms_ 01.pdf, [Mar. 5, 2018].

[15] B. E. Anderson. "Derivation of Moving-Coil Loudspeaker Parameters Using Plane Wave Tube Techniques." Master's thesis, Brigham Young University, US, 2003.

[16] V. Dickason. *Loudspeaker Design Cookbook*, 7th edition. Chase City, VA: KCK Media Corp. 2006, pp. 12.

[17] T. Söderström, P. Stoica. *System Identification*. Hertfordshire, UK: Prentice Hall International, 1989, pp. 188-192.

[18] L. Ljung. *System Identification: Theory for the User.* Upper Saddle River, NJ: Prentice-Hall PTR, 1999.

[19] T. S. Hsu, K. A. Poornima. "Loudspeaker failure modes and error correction techniques." *Applied Acoustics*, vol. 62, pp. 717-734, Jul. 2000.

[20] W. Klippel, J. Schlechter. "Fast Measurement of Motor and Suspension Nonlinearities in Loudspeaker Manufacturing ." Internet: https://www.klippel.de/fileadmin/klippel/Files/Know_How/Literature/ Papers/Fast%20Measurement%20of%20Motor%20and%20Suspension% 20Nonlinearities.pdf, [Mar. 5, 2018].

[21] W. Klippel. "Assessing Large Signal Performance of Transducers." Internet: https://www.klippel.de/fileadmin/klippel/Files/Know_How/Literature/ Papers/Assessing_the_large_Signal_performance_of_Loudspeakers_02.pdf, [Mar. 5, 2018].

[22] W. Klippel. "Distortion Analyzer - a New Tool for Assessing and Improving Electrodynamic Transducer." Internet: https://www.klippel.de/fileadmin/klippel/Files/Know_How/Literature/ Papers/Distortion_Analyzer_a_New_Tool_00.pdf, [Mar. 5, 2018].